Eur. J. Mech. B/Fluids, **18**, n° 2, 261-282, 1999

On the effectiveness and limitations of local criteria for the identification of a vortex

R. CUCITORE, M. QUADRIO, A. BARON *

ABSTRACT. – Three proposed local criteria for the identification of vortices are analyzed and discussed; they are based on the analysis of invariants of the velocity gradient tensor $\nabla \mathbf{u}$ or invariants of the tensor $\mathbf{S}^2+\mathbf{\Omega}^2$, where $\mathbf{S}$ and $\mathbf{\Omega}$ are the symmetric and antisymmetric parts of $\nabla \mathbf{u}$.

Moreover, a tentative non-local procedure is proposed, which takes advantage of the observation that vortices tend to be made up of the same fluid particles; this leads to the definition of a Galilean invariant quantity, which can be computed and used to identify vortical structures.

Three analytical flow fields are used for a comparative evaluation of both local and non-local criteria, which allows a deeper understanding of the physical meaning of the considered techniques. © Elsevier, Paris.

Keywords. – Vortices, identification.

1. Introduction

Although the concept of a vortex occurs in nearly every branch of fluid dynamics, an agreed definition for such a basic structure does not yet exist. The attention of fluid dynamics researchers started to increase when, several years ago, it was experimentally proved that the presence of organized structures was important in many turbulent flows, which would otherwise seem chaotic. Such structures, so-called coherent structures, are at the base of all the attempts to explain the physics of turbulent motions, and the assumption that the constitutive elements of coherent structures can be considered vortices is well accepted (Cantwell, 1981; Hussain, 1986; Robinson, 1991).

The growing interest in turbulent flows is increasing the necessity for a definition, or at least for a working definition, of vortices. This could lead to improvements in basic research in turbulence physics, and, consequently, to developments of either turbulence modeling or active/passive control techniques for boundary layers. Among other things, it could also profit the design of high-lift devices or delta wings. Recently, the impressive developments of direct numerical solution of the Navier-Stokes equations for the modeling of turbulent flows, and the parallel improvement of experimental techniques, have led to a high availability of huge databases. The opportunity of having all the flow details known in principle, has even further increased the need for a black-box algorithm that, given a flow field, could immediately identify and highlight the structures contained therein, thus allowing one to follow their evolution once a time series of flow fields is available. A recent and notable example is offered in the paper by Jeong *et al.* (1997).

Following Jeong and Hussain (1995), we recognize that the spatial extent of a vortex in a viscous fluid depends on the threshold selected by the identifier, and, according to the usual practice, in this paper we will limit ourselves to identifying the cores of vortical structures (hence the words *vortex* and *vortex core* will be

Politecnico di Milano, Dipartimento di Ingegneria Aerospaziale, via La Masa 34, Milano 20158, Italy.
* Correspondence and reprints.

0997-7546/99/02/© Elsevier, Paris

used without distinction). As suggested by Jeong and Hussain (1995), a vortex should at least possess the following properties:

(i) a vortex core must have a net vorticity, and consequently a net circulation. Potential flow regions are excluded from vortex cores by this requirement, and a potential vortex is a vortex with zero cross-section;

(ii) the geometrical characteristics of the identified vortex core must be Galilean invariant.

In spite of these prerequisites, there is no single solution to the problem of vortex identification. The simplest procedures are based on the search for regions of the flow field characterized by some property, intuitively related to a vortical motion. More recently, three additional definitions of a vortex have been proposed, by Chong *et al.* (1990), Hunt *et al.* (1998), and Jeong and Hussain (1995). All of them are based on the analysis of the velocity gradient tensor $\nabla \mathbf{u} = u_{i/j}$ (the subscript $/j$ denotes differentiation). These definitions are Galilean invariant, and are based on less intuitive physical considerations.

The issue of vortex identification is by no means trivial, and in fact several of the existing techniques can give good results in many situations, but all of them can be shown to fail (or, at least, to produce ambiguous answers) in particular conditions.

The main existing vortex definitions will be briefly reviewed in the next section, with emphasis on those based on the analysis of the velocity gradient tensor, and with particular attention to their physical foundation. The paper by Jeong and Hussain (1995) deserves special attention, firstly since it is the most recent, and secondly since it describes one of the most promising techniques, citing several examples. In our paper we will follow its overall structure, and henceforth it will be referred to as JH. In section 3 we will add some additional contribution to the issue of vortex identification, emphasizing in particular the need for a non-local analysis. Section 4 will contain a comparative application of all the definitions, with a critical analysis of the results.

2. Analysis of previously proposed definitions

After giving a short summary of the techniques denoted as *intuitive* by JH, the three recently proposed criteria based on the analysis of the velocity gradient tensor $\nabla \mathbf{u} = u_{i/j}$ will be examined. They all satisfy the requirements (i) and (ii) outlined in section 1. It is explicitly noted by JH that in planar flows these three criteria are fully equivalent.

2.1. Intuitive definitions

Several authors (see for example Spalart, 1988) use the magnitude of the vorticity vector ω, as an indicator of vortical structures. It must be said, however, that the use of $|\omega|$ may be misleading: it may fail, for example, in wall-bounded flows, because $|\omega|$ cannot distinguish between rotation due to pure shear and rotation due to an actual swirling motion. Consequently, problems arise when $|\omega|$ due to the background shear becomes comparable to that due to a swirling motion (the simple Couette flow is a clear example of high values of $|\omega|$ not corresponding in any way to vortical motion). Even in free shear flows, JH show how the vorticity magnitude is not an adequate criterion for the identification of vortices.

Another frequently used scalar indicator of vortical motion is pressure (Kline and Robertson, 1990). With a steady inviscid planar two-dimensional flow, in fact, in the case of rotating motion the pressure shows a minimum at the center of the circular pattern. This is simply a consequence of the balance of the forces acting on a fluid element in the radial direction; the centrifugal force must be balanced by the force due to a radial pressure gradient, which is responsible for the minimum on the axis of the rotation. However when the flow is unsteady, viscous, or three-dimensional, this is no longer true, as JH show in their examples. In the case of Karman's viscous pump, because of viscous effects the pressure has no minimum on the axis near the wall,

while the motion is clearly vortical. An unsteady, inviscid flow is then presented by JH, where because of unsteadiness the pressure has a well-defined minimum on the axis of a clearly non-rotating motion.

It is commonly accepted that vortical structures are basically characterized by a swirling motion, in a suitable reference frame, and in fact their presence has been widely associated with the presence of closed or spiral streamlines or pathlines. It is evident that these methods of identifying vortices do not prove to be Galilean invariant. Besides, as shown by JH, there is the problem that a particle must complete a full revolution around the vortex center, in order to have a circular streamline or pathline, and this is not always the case in the presence of highly unsteady flows.

2.2. Complex eigenvalues of $\nabla \mathbf{u}$

Chong *et al.* (1990) also propose a criterion for identifying vortices which refers to the presence of circular or spiral streamlines (see also Perry and Chong, 1987, for additional details). Moreover, they are able to bypass the problems of non Galilean invariance and unsteadiness. Their technique consists of verifying the curvature of the streamlines at any point in the flow field, but in a local reference frame, moving at the velocity of that point, in order to get an actual Galilean invariant procedure. In order to achieve this purpose, there is no need for an explicit integration of the equations for the streamline pattern, since the same information can be gathered from the analysis of the eigenvalues of the velocity gradient tensor $\nabla \mathbf{u} = u_{i/j}$ at the same point. A region of complex eigenvalues for $\nabla \mathbf{u}$ is then defined as a vortex, since complex eigenvalues imply that the local streamline pattern is closed or spiral in a reference frame that moves with the point. As the authors point out, this is equivalent to having the antisymmetric part of $\nabla \mathbf{u}$ prevailing over the symmetric one.

The eigenvalues σ of $\nabla \mathbf{u}$ satisfy the characteristic equation:

$$\sigma^3 - P\sigma^2 + Q\sigma - R = 0, \tag{1}$$

where P, Q and R are the three invariants of $u_{i/j}$ and are defined as follows:

$$P = u_{i/i}, \qquad Q = \frac{1}{2}(u_{i/i}^2 - u_{i/j}u_{j/i}), \qquad R = \det(u_{i/j}).$$

Complex eigenvalues will occur when the discriminant Δ of (1) is positive; in the case of incompressible flow, where $P = 0$, this leads to the condition:

$$\Delta = \left(\frac{1}{3}Q\right)^3 + \left(\frac{1}{2}R\right)^2 > 0.$$

2.3. The second invariant $\nabla \mathbf{u}$

Hunt *et al.* (1988) define vortices as regions where the second invariant Q of the tensor $\nabla \mathbf{u}$ is positive, with the additional condition that the pressure is lower than the ambient value.

Unlike the previous method, this requires the additional condition of low pressure, and it is possible to show that this condition is independent of the sign of Q. In fact, from the Navier–Stokes equations, the Poisson equation for the pressure can be written in terms of Q as:

$$\nabla^2 p = 2\rho Q.$$

The maximum principle applied to this equation states that pressure maxima can occur only on the boundary if $Q \geq 0$ and the pressure minima can occur only on the boundary if $Q \leq 0$. However, $Q \geq 0$ does not necessarily imply that pressure minima occur within the region. Thus there is no explicit connection between a region with $Q \geq 0$ and a region containing a pressure minimum.

2.4. Two negative eigenvalues for $\mathbf{S}^2 + \mathbf{\Omega}^2$

JH define, for a constant-property fluid, a vortex core as a connected region where the tensor $\mathbf{S}^2 + \mathbf{\Omega}^2$ has two negative eigenvalues. The tensors $S_{ij} = 1/2(u_{i/j} + u_{j/i})$ and $\Omega_{ij} = 1/2(u_{i/j} - u_{j/i})$ are the symmetric and antisymmetric components of $\nabla \mathbf{u}$. The authors' rationale is to improve the performance of the criterion based on the search for pressure minima, described in section 2.1, by overcoming the causes of its failure, i.e. unsteady straining and viscous effects.

Taking the gradient of the Navier–Stokes equations, they derive the equation:

$$a_{i/j} = -\frac{1}{\rho} p_{/ij} + \nu u_{i/jkk}, \tag{2}$$

where $a_{i/j}$ is the acceleration gradient and the symmetric tensor $p_{/ij}$, the Hessian of the pressure, contains information on local pressure extrema. Then, $a_{i/j}$ can be broken down into a symmetric and an antisymmetric part as follows:

$$a_{i/j} = \left[\frac{\mathrm{D}S_{ij}}{\mathrm{D}t} + \Omega_{ik}\Omega_{kj} + S_{ik}S_{kj}\right] + \left[\frac{\mathrm{D}\Omega_{ij}}{\mathrm{D}t} + \Omega_{ik}S_{kj} + S_{ik}\Omega_{kj}\right].$$

The symmetric part of (2) is therefore:

$$\frac{\mathrm{D}S_{ij}}{\mathrm{D}t} - \nu S_{ij/kk} + \Omega_{ik}\Omega_{kj} + S_{ik}S_{kj} = -\frac{1}{\rho} p_{/ij}. \tag{3}$$

If $p_{/ij}$ has two positive eigenvalues, there is a local pressure minimum on the plane of the two eigenvectors associated with those eigenvalues.

The first term on the left-hand side of (3) represents unsteady irrotational straining and the second term represents viscous effects. Thus, considering only $\mathbf{S}^2 + \mathbf{\Omega}^2$ allows one to determine the existence of a local pressure minimum due to vortical motion.

Note that since the tensor $\mathbf{S}^2 + \mathbf{\Omega}^2$ is symmetric, it has only real eigenvalues. If we assume that the eigenvalues are ordered, in such a way as:

$$\lambda_1 \geq \lambda_2 \geq \lambda_3, \tag{4}$$

we conclude that this criterion is equivalent to requiring $\lambda_2 < 0$; hence this technique is also referred to as the λ_2-definition.

In the case of a compressible flow, the same procedure can be repeated in order to obtain the expression for the Hessian of the pressure. Obviously, additional terms arise due to non-zero density gradients and to the non-zero trace of $\nabla \mathbf{u}$. For a complete derivation of these expressions we refer to the appendix. It has to be noted that, in the case of a compressible flow, the equivalence of the methods based on the analysis of the velocity gradient tensor for two-dimensional flows is no longer valid.

3. Some additional contribution to the issue of vortex identification

3.1. Considerations on the methods based on the analysis of $\nabla \mathbf{u}$

It is possible to see how the tensors $\mathbf{S}$ and $\mathbf{\Omega}$, used in the λ_2-definition, play a role also in the criterion proposed by Hunt *et al.* (1988). With this aim, let us rewrite the second invariant Q of the velocity gradient tensor as:

$$Q = \frac{1}{2}(\|\mathbf{\Omega}\|^2 - \|\mathbf{S}\|^2), \tag{5}$$

where $\|\mathbf{S}\| = [\mathrm{tr}(\mathbf{S}\mathbf{S}^T)]$ and $\|\mathbf{\Omega}\| = [\mathrm{tr}(\mathbf{\Omega}\mathbf{\Omega}^T)]$.

It can be useful to rewrite equation (5) making evident the dependence of Q on the components of $\mathbf{S}$ and $\mathbf{\Omega}$, as follows:

$$Q = (\omega_1^2 + \omega_2^2 + \omega_3^2) - \left[(\gamma_1^2 + \gamma_2^2 + \gamma_3^2) + \frac{1}{2}(\epsilon_1^2 + \epsilon_2^2 + \epsilon_3^2)\right], \tag{6}$$

where:

$$\begin{aligned} \omega_1 &= \Omega_{32} = -\Omega_{23} \\ \omega_2 &= \Omega_{13} = -\Omega_{31} \\ \omega_3 &= \Omega_{21} = -\Omega_{12} \end{aligned}$$

$$\begin{aligned} \gamma_1 &= S_{32} = S_{23} \\ \gamma_2 &= S_{13} = S_{31} \\ \gamma_3 &= S_{21} = S_{12} \end{aligned}$$

$$\begin{aligned} \epsilon_1 &= S_{11} \\ \epsilon_2 &= S_{22} \\ \epsilon_3 &= S_{33}. \end{aligned}$$

The relations (5) or (6) show that the quantity Q represents a local balance between the rotation and deformation rates of a fluid element. Hence this technique essentially uses the same definition of a vortex as that formulated by Chong *et al.* 1990: a vortex is a connected region where the antisymmetric component of $\nabla \mathbf{u}$ predominates over the symmetric one.

If we turn now to the JH paper and λ_2-definition, they present the procedure for the identification of vortices as basically derived from the criterion of pressure minima (briefly described in section 2.1), enhanced by removing the main causes of inaccuracy, i.e. unsteady straining and viscous effects. However it is possible to give another physical explanation to this criterion. We know (from JH and Thuesdell, 1953) that Q equals the opposite of the half-sum of the three eigenvalues of $\mathbf{S}^2 + \mathbf{\Omega}^2$. This suggests that the present criterion operates by locally comparing strain to rotation. It is possible to see in which way this is made, by writing $\mathbf{S}^2 + \mathbf{\Omega}^2$ in a reference frame where each axis is parallel to an eigenvector of the tensor, with x_1 the direction parallel to the vortex axis. In such a reference frame the tensor itself can be expressed as a diagonal matrix, and can be written in the following form:

$$\mathbf{S}^2 + \mathbf{\Omega}^2 = \begin{bmatrix} \mathrm{grad}(u_1) \cdot \mathbf{u}_{/1} & 0 & 0 \\ 0 & \mathrm{grad}(u_2) \cdot \mathbf{u}_{/2} & 0 \\ 0 & 0 & \mathrm{grad}(u_3) \cdot \mathbf{u}_{/3} \end{bmatrix}.$$

The diagonal elements can be rewritten as follows:

$$\begin{aligned} \text{grad}(u_1)\cdot\mathbf{u}_{/1} &= [\epsilon_1^2+(\gamma_2^2+\gamma_3^2)]-(\omega_2^2+\omega_3^2)=\lambda_1 \\ \text{grad}(u_2)\cdot\mathbf{u}_{/2} &= [\epsilon_2^2+(\gamma_1^2+\gamma_3^2)]-(\omega_1^2+\omega_3^2)=\lambda_2 \\ \text{grad}(u_3)\cdot\mathbf{u}_{/3} &= [\epsilon_3^2+(\gamma_1^2+\gamma_2^2)]-(\omega_1^2+\omega_2^2)=\lambda_3. \end{aligned} \tag{7}$$

Requiring the intermediate eigenvalue λ_2 to be < 0 is then equivalent to requiring that some measure of rotation rate prevails over some measure of the deformation rate. In a vortex with its axis aligned with the x_1 direction, it must have $\lambda_2 < 0$ and $\lambda_3 < 0$. It follows that ω_1^2 must be sufficiently greater than γ_1^2, in order for λ_2 to be negative. The possibility that $\lambda_3 < 0$ because of ω_2^2, and that $\lambda_2 < 0$ because of ω_3^2 is excluded by the validity of the ordering relation (4) between the eigenvalues.

From (7), it can be seen that even the criterion proposed by JH, as well as that of Hunt *et al.* (1988), essentially uses the same vortex definition as that of Chong *et al.* (1990), carrying out the balance between shear and rotation rates in the plane normal to the vortex axis (at least the vortex axis selected according to the present method). An important difference from the criterion of Hunt *et al.* (1988) is that this method is able by itself to obtain the information on the direction of the vortex axis from the analysis of the tensor $\mathbf{S}^2+\mathbf{\Omega}^2$.

3.2. A PROPOSAL FOR A NON-LOCAL ANALYSIS

All the methods based on the analysis of the velocity gradient tensor, presented in the preceding sections, are characterized (and sometimes limited) by their common property of performing local analyses of the flow field. This means that they cannot relate the behavior of a fluid element to the behavior of other fluid elements lying in a region of space of extension comparable with the spatial extension of the vortex.

On the other hand, it is not unreasonable to expand the basic requirements for a vortex, put forward in section 1, by adding the idea of vortices as *structures*: the concept of *non-locality* is so introduced.

We are certainly facing the usual problem of knowing nothing about the mechanism by which a coherent, vortical structure drives the motion of a fluid parcel; nevertheless, searching locally by carrying out a purely local analysis implies giving up *a priori* additional information, available only to non-local investigation procedures. However, if we knew more about the particular nature of the structure, a local analysis would be sufficient to identify vortices.

The simple search for closed or spiral pathlines (or streamlines), as seen in section 2.1, is a non-local procedure, but it is also non-Galilean invariant. In this section, we will try to outline a possible, Galilean invariant, non-local analysis, by using the intuitive notion (confirmed by experience) that the particles inside a vortical structure show small variations in their relative distance even when following completely different trajectories.

Let us consider a couple (a,b) of particles in a flow, where we define *particles* as points whose position satisfies the equation of motion:

$$\frac{d\mathbf{x}}{dt}=\mathbf{u}(\mathbf{x},t). \tag{8}$$

Let $\mathbf{u}_a$ and $\mathbf{u}_b$ be their respective velocities, and let us introduce the ratio:

$$R(\mathbf{x},t)=\frac{\left|\int_0^t \mathbf{u}_a(\tau)d\tau-\int_0^t \mathbf{u}_b(\tau)d\tau\right|}{\int_0^t |\mathbf{u}_a(\tau)-\mathbf{u}_b(\tau)|d\tau}. \tag{9}$$

The numerator of (9) measures the evolution of the relative distance between the two particles from time zero to time t, while the denominator is a measure of the difference of the particle trajectories in the same time interval, since the integrand is the modulus of the relative velocity between the two particles. The quantity R, which is function of time t and $\mathbf{x}$ (the mid point between $\mathbf{x}_a$ and $\mathbf{x}_b$), is bound between 0 and 1 and its key property is that it assumes lower values for pairs of particles belonging to a vortical structure, while reaching high values for pairs outside the structures. Moreover, $R(\mathbf{x}, t)$ is a Galilean invariant quantity, hence satisfying requisite (ii) of section 1; the requisite (i) must be explicitly demonstrated.

In order to clarify the physical meaning of the quantity R, let us first consider the Couette flow, where the denominator of (9) grows linearly with time, and the numerator grows in the same way, so that $R \equiv 1$. Hence the quantity R, unlike the methods based on $|\omega|$, is capable of discriminating between background shear and vortical motion. Moreover, it can be seen that $R \equiv 1$ also in pure radial flows. In the case of pairs of particles placed inside a vortical structure, the denominator of (9) grows indefinitely with time, the trajectories being completely different, while the numerator has a slower growth, since the particles do not greatly change their relative distance, as long as they remain inside the vortical structure.

As a further example, figure 1(a,b) shows the behavior of the quantity $R(t)$ for the schematic case of two particles (marked with a circle and an asterisk in the figure) subjected first to a solid-body rotation superimposed on a constant advection. At the time instant t_c the rotation is suddenly switched off, and a pure Couette motion is started. Figure 1(a) shows a sketch of the motion, while figure 1(b) describes the behavior of the quantity $R(t)$ with time; it can be seen that while $t < t_c$ $R(t)$ decreases towards zero; when Couette motion is started, $R(t)$ starts increasing slowly and eventually tends to its asymptotic value of unity.

In the following section, we will compute the ratio $R(t)$ by using a single flow field, i.e. by supposing the flow as frozen at a particular point in time, so that t does not indicate physical time anymore, but only a parameter. This allows an immediate comparison of the results with those obtained by the other methods, which all operate at a given time. In this way, the interpretation of the results is easier, the possible effects of dynamical evolution of the flow being absent.

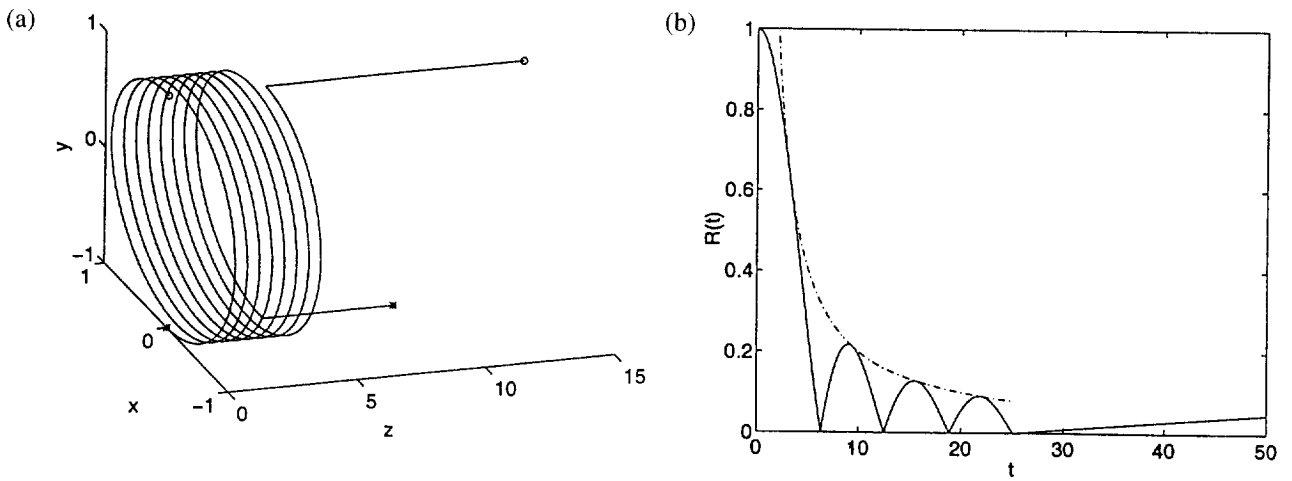

Fig. 1. – Computation of the quantity $R(t)$ for a model flow. (*a*) Illustration of two particles first subjected to circular helical motion with the angular velocity vector parallel to the z axis, for $t < t_c$; the rotating motion is switched off at pseudo-time $t = t_c$, after which a pure Couette motion is started with one particle moving twice as fast as the other. (*b*) Behavior of the quantity R as a function of time; the bounding hyperbole has equation $2/(\omega t)$, where ω is the modulus of the angular velocity vector of the helical motion; computations are performed with $\omega = 1$ and $t_c = 25.133$, which corresponds to 4 rotations.

The overall procedure of analysis can be summarized as follows. Firstly, a large number of particles is considered at random positions in a flow field. A (possibly high) number of pairs is then identified, whose relative distance belongs to the interval $[d_m, d_M]$. Note that a single particle can be considered to belong to more than one pair, so that the number of pairs can be larger than the number of particles. The interval $[d_m, d_M]$ can be freely determined, and this is a filtering feature of the procedure, for the results will not contain information on structures whose spatial scale is smaller than d_m. Such a feature can be interesting when dealing with complex turbulent flow fields (for example those computed by a DNS of Navier–Stokes equations), where the spatial scale and location of the vortical structures are not known in advance.

Secondly, a value for the pseudo-time t has to be specified. This choice turns out not to be crucial, but it is important to observe that, if t is too high, some information can be lost: with reference to figure 1(b), it can be seen that the integration time cannot be arbitrarily high. Physical considerations can help in setting the optimum value for t, and it must be recalled that usually the rate at which the quantity $R(t)$ starts increasing after the particles have been distanced from the vortex core is quite low (this is evident from the analysis of figure 1(b)).

The ratio $R(t)$ can then be evaluated for every pair, and followed in pseudo-time by integrating the equation (8) describing its trajectory.

The results can eventually be plotted on a graph by choosing a threshold value R_{th}, and by plotting in the flow field only the position of the couples of particles with $R(t) \leq R_{th}$, or, better, the position of the midpoint between the two particles at the instant $t = 0$.

3.3. A REMARK ON THE DEFINITION BASED ON Δ

The definition of vortices as regions where the scalar Δ is positive presents the drawback, highlighted by JH, of being unable to treat cases where the streamline pattern becomes locally closed or spiral, without the presence of a truly vortical structure (see figure 6*c,d* of JH).

However, there is no doubt that the overall nature of motion in vortical regions with $\Delta > 0$ presents differences from non-vortical regions with $\Delta > 0$. It is reasonable to think of vortices as structures which tend to be made up of the same fluid elements. Consequently, particles put in a truly vortical region with positive Δ tend to remain in a region characterized by positive Δ. On the contrary, if the region with $\Delta > 0$ has no vortical motion, particles put there will probably migrate quickly towards regions with $\Delta < 0$.

A possible complement to the identification of vortices purely based on the sign of Δ consists in analyzing the variation in time of the number of particles present in a particular region with positive sign of Δ. About this procedure, we can make the same remarks as those put forward in section 3.2 regarding the use of a single flow field and the integration at fixed physical time; whenever the number of particles shows a clear tendency to decrease, the identified region with positive Δ cannot be considered as a truly vortical structure. It is clear that, if the choice of the integration time has no relevance in steady flows (as shown in section 4.1), it becomes crucial in unsteady flows. In these cases, the dynamical evolution of the flow field, which leads for example to the interaction between two structures initially separated or to the creation of new structures, may increase the difficulty in interpreting the results.

4. Comparative application of criteria to analytical flow fields

In this section three analytical flow fields will be selected, in order to evaluate the previously presented methods for vortex identification. One of the flow fields has been derived expressly for the present work; the second one (the Bödewadt vortex) has been used also by JH; the third one (the tornado flow), like the apparently similar flow used by JH, is a conically-symmetric solution of the Navier–Stokes equations.

The dynamical significance of vortical structures is not investigated here; our attention is rather focused on their objective detection. The techniques presented in the previous sections are, for convenience, summarized below:

- Δ-*definition*: the region of complex eigenvalues for $\nabla \mathbf{u}$.
  The boundary of this region is given by the surface:
$$\Delta = \left(\frac{1}{3}Q\right)^3 + \left(\frac{1}{2}R\right)^2 = 0$$
  (the surface with $\Delta = 0$ is excluded).
- *Q-definition*: the region of positive
$$Q = \frac{1}{2}(u_{i/i}^2 - u_{i/j}u_{j/i}) = \frac{1}{2}(\|\mathbf{\Omega}^2\| - \|\mathbf{S}^2\|)$$
  with the additional condition of low pressure (surface with $Q = 0$ is excluded).
- λ_2-*definition*: the region of negative second largest eigenvalue for the tensor $\mathbf{S}^2 + \mathbf{\Omega}^2$ (surface with $\lambda_2 = 0$ is excluded).
- *R-definition*: the region identified by pairs of particles with R less than a threshold value.

The first three definitions will be considered sequentially, while the R-definition will be used in each of the following sections, in order to compare its results with those obtained by using the other techniques.

4.1. Application of Δ-definition

4.1.1. *Model for a tornado*

This flow, described in detail in Shtern and Hussain (1993) and further studied in Shtern and Hussain (1996), is generated by a swirling jet flowing out normal to a plane, and possessing a source of axial momentum at the origin. The velocity field presents a conical symmetry, and in spherical coordinates it can be written as:

$$u_r = -\nu\frac{\psi'(c)}{r}; \qquad u_\theta = -\nu\frac{\psi(c)}{r\sin\theta}; \qquad u_\phi = \nu\frac{\Gamma(c)}{r\sin\theta} \tag{10}$$

where θ and ϕ are the polar and azimuthal angles respectively, r is the distance from the origin, $c = \cos\theta$, and $\Gamma(c)$ and $\psi(c)$ are two unknown functions. The flow satisfies the full Navier–Stokes equations; the non-dimensional functions $\Gamma(c)$ and $\psi(c)$ can be determined with a numerical algorithm suggested by Shtern and Hussain (1993). In their paper they carry out an asymptotic analysis for Γ_0, which is defined as $\Gamma(0)$ and can be seen as a swirl Reynolds number, tending to infinity. The asymptotic solution corresponds to the sketch shown in figure 2(a) (two-cell flow). Equations (10) also admit a one-cell solution, illustrated in figure 2(b), which is used by JH in their paper.

In their analysis Shtern and Hussain assume thin layers (where viscous effects cannot be ignored) near the z-axis ($c = 1$), near the plane $\theta = \pi/2$ ($c = 0$) and near the cone $\theta = \theta_s$ ($c = c_s$). In the regions separating these layers, viscous effects are considered negligible, and the authors calculate the functions ψ and Γ in those regions by solving the Euler equation for conical flows. The analytical expressions for Γ and ψ are:

$$\begin{cases} \Gamma(c) = \Gamma_0, \qquad \psi(c) = \Gamma_0\sqrt{\dfrac{c[2c_s - (1+c_s)c]}{(1+c_s)}} & \text{if } 0 \le c < c_s \\ \Gamma(c) = 0, \qquad \psi(c) = -\Gamma_0\dfrac{c_s(1-c)}{\sqrt{1-c_s^2}}, & \text{if } c_s < c \le 1\,. \end{cases} \tag{11}$$

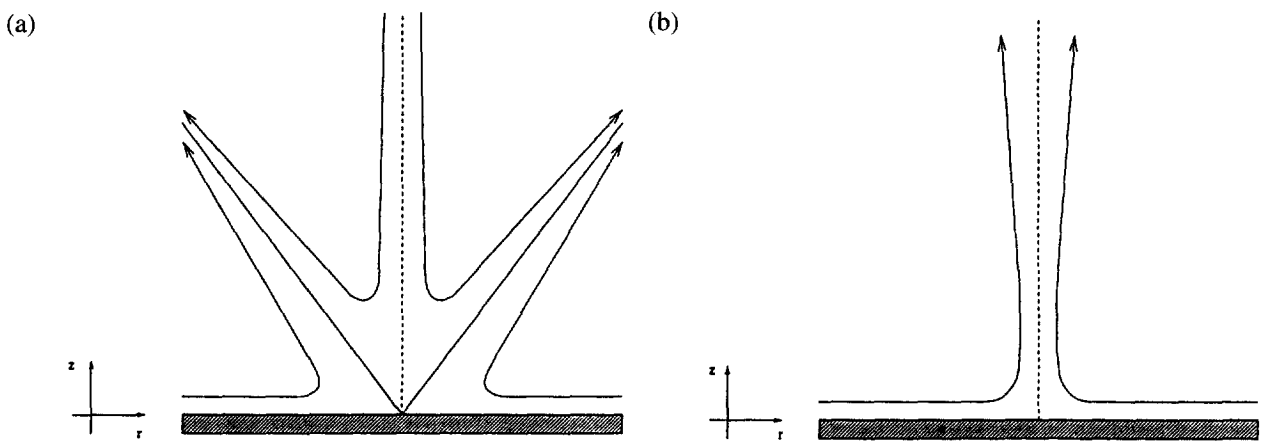

Fig. 2. – Illustration of the meridional motion in the tornado model flow, after Shtern and Hussain (1993): (*a*) two-cell patterns; (*b*) one-cell patterns.

The full Navier–Stokes solution is singular at the point $r = 0$, while the Euler solution, expressed by (11), is singular on the plane $c = 0$ (containing the point $r = 0$). Figure 3 shows the meridional motion in the flow field, by plotting the Stokes streamfunction $\Psi(c) = \nu r \psi(c)$. It has to be noted that the streamlines approaching the conical surface $\theta = \theta_s$ are not tangent to the conical surface itself; the velocity vectors for $\theta \to \theta_s^-$ and $\theta \to \theta_s^+$ have both the same magnitude and direction, but opposite sign. From a physical point of view, a sink distribution is present on the surface $\theta = \theta_s$ which implies that mass is not conserved in the inviscid solution of the flow. Despite the difficulties implied by the presence of this discontinuity, the inviscid solution has been preferred to the (continuous) viscous solution because of the existence of an exact solution for the velocity field which allows us both to use analytical forms for the spatial derivatives and to avoid interpolation in the particle path computation. The vorticity components (Shtern and Hussain, 1993) are:

$$\omega_r = -\nu \frac{\Gamma'(c)}{r^2}, \qquad \omega_\theta = 0, \qquad \omega_\phi = -\nu \frac{\psi''(c)}{r^2}.$$

In this asymptotic case the only non-zero vorticity component is ω_ϕ, in the region $0 \leq c < c_s$. In order to avoid numerical inaccuracies near the plane $z = 0$ and the cone $\theta = \theta_s$, all the derivatives necessary for the application of the definitions recalled in section 2 are analytically evaluated.

The application of Δ-definition to this flow field is illustrated in figure 4. For the computations, the value $c_s = 0.9$ is used, and $\nu\Gamma_0$ has been set to 50 (these parameters remain the same also in the other computation of this model flow). Δ understands the geometry of the conical vortex structure, showing a thin region with positive values where the vortex core is identified, bounded by the cone $\theta = \theta_s$ and by a second cone at a slightly larger polar angle. This confirms the observation made by Jeong and Hussain (1995) that Δ tends to overestimate the size of the vortex cores. However in addition to this, far from the z axis Δ evidences a second region with positive values. This is due to the known limitation of Δ, which is not able to treat some cases with locally closed or spiral streamline patterns.

In section 3.3 we have suggested a possible way of interpreting the results of an analysis based on Δ, in order to be able to discriminate truly vortical regions with $\Delta > 0$ from regions with $\Delta > 0$ but without vortical organization. As mentioned above (figure 3), the streamlines converge towards the vortical region at $\theta = \theta_s$ anywhere in the field (see figure 2(a) for the general description of the flow field), so that particles put in the region with $\Delta > 0$ near $\theta = \theta_s$ cannot enter the region with $\Delta < 0$. It follows that they either remain in the $\Delta > 0$ region or, when they reach the surface $\theta = \theta_s$, are extracted from the flow field by the sucking action of

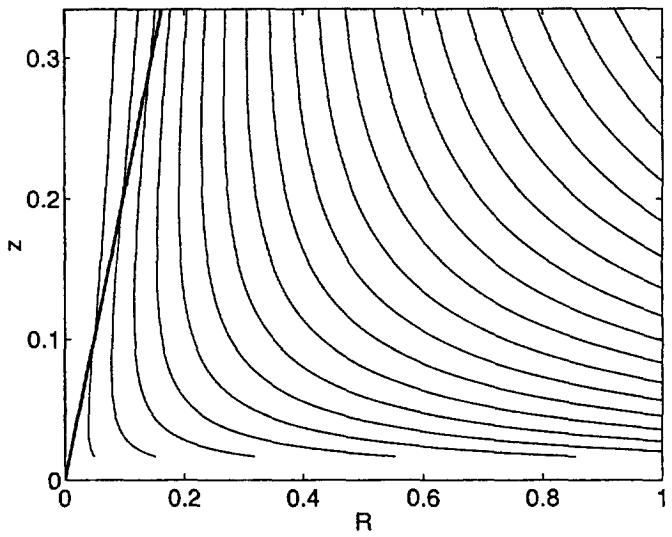

Fig. 3. – Contours of Stokes streamfunction Ψ for the tornado flow, with $c_s = 0.9$ and $\nu\Gamma_0 = 50$. The singular plane $z = 0$ is excluded from the plot. Thick line corresponds to $\theta = \theta_s$.

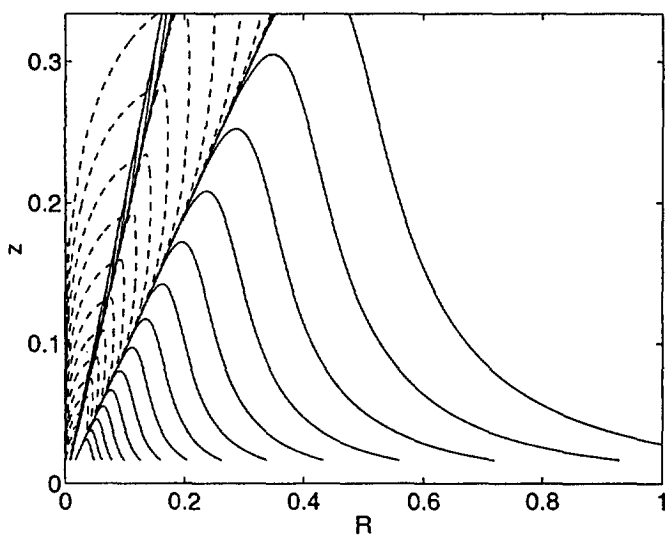

Fig. 4. – Contours of Δ for the tornado flow, with $c_s = 0.9$ and $\nu\Gamma_0 = 50$. The singular plane $z = 0$ is excluded from the plot. Continuous lines represent positive levels, and dotted lines represent negative levels. The level zero is plotted as a continuous line.

the sink distribution. On the other hand, the particles which have been put in the second region with positive Δ tend to exit, as can be seen in figure 3. Consequently, the number of particles decreases in pseudo-time, as shown in figure 5; this indicates that the present region cannot be regarded as a truly vortical structure.

The results of the computation of the quantity $R(t)$ are illustrated in figure 6(a,b,c). Figure 6(a) has been obtained by using the flow field shown in figure 3 and putting in a slice, 0.5 thick, 12,000 particles. Pairs of particles with relative distance between $d_m = 0$ and $d_M = 0.08$ have then been selected: the initial number of pairs was around 18,000. After the computation performed with 500 time steps for 0.0075 pseudo-time units, the location of the mid point of the particle pairs is reported in figure 6(a), by excluding the pairs collapsed into the surface $\theta = \theta_s$ but plotting all the others (i.e. $R_{th} = 1$). The number of pairs in the flow field at time

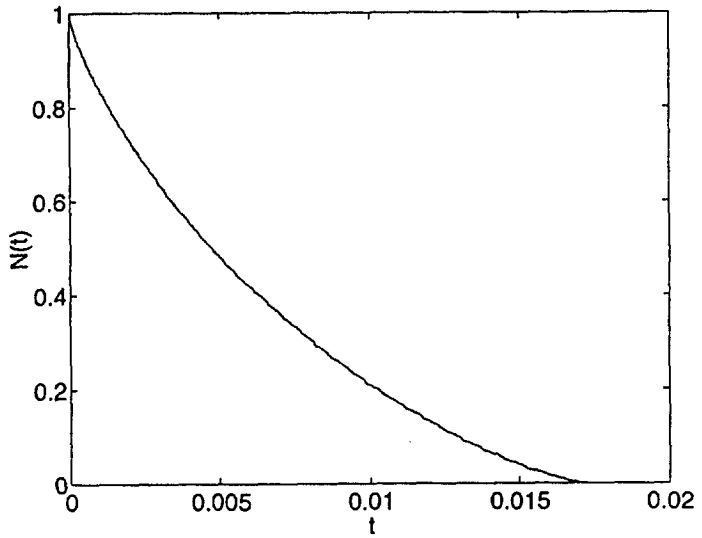

Fig. 5. – Normalized variation with t of the number of particles put in the lower region of figure 4 with $\Delta > 0$. At $t = 0$ the number of particles is 1276.

$t = 0.0075$ is 15,000 and a particle-free region is obviously generated in the proximity of $\theta = \theta_s$ surface. The thickness of the particle-free region increases with the pseudo-temporal integration interval: the final results, however, remain unchanged.

For R_{th} equal to 0.98 the number of particle pairs having $R < R_{th}$ is 920; the spatial distribution of the pairs is illustrated in figure 6(b) and it seems to indicate the presence of a vortical region only for θ values larger than θ_s. The relatively limited number of particles located in the region defined by $\theta < \theta_s$ must in fact be discarded according to the $|\omega|$ condition (see section 3.2). It has to be noted, however, that for a threshold value as high as 0.93 no particle pairs are detected in the irrotational region. The sensitivity of the method to the threshold value R_{th} has been investigated in the present case; figure 6(c) reports the case of $R_{th} = 0.995$, where despite the large value of R_{th} the overall appearance of the vortex structure is still well defined (the number of the selected pairs is approximately 2,400 in this case).

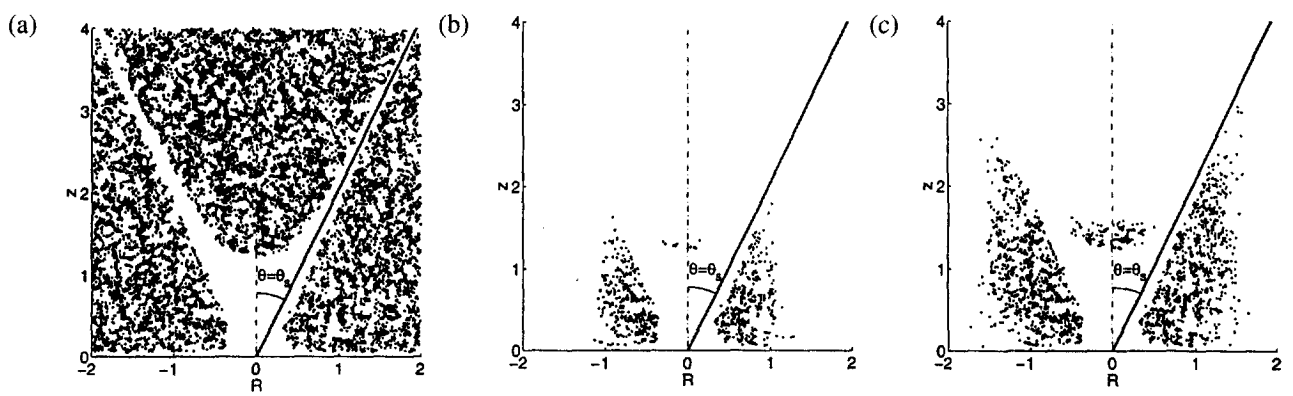

Fig. 6. – Initial positions of the mid point of particle pairs with $R < R_{th}$ for the tornado flow. The integration period is $t = 0.015$, $c_s = 0.9$ and $\nu\Gamma_0 = 50$. Pairs followed in pseudo-time are 18029. (*a*) 15227 pairs have $R \leq R_{th} = 1$; (*b*) 920 pairs have $R < R_{th} = 0.98$; (*c*) 2397 pairs have $R < R_{th} = 0.995$.

4.1.2. *An unsteady inviscid radially stretched vortex*

This flow field constitutes an exact solution of the Euler equation, determined *ad hoc* as a further test case for the methods examined here. The solution has, in cylindrical coordinates, the following form:

$$u_r = -\alpha(t)r, \qquad u_\theta = c(t)r^a, \qquad u_z = 2\alpha(t)z, \tag{13}$$

where z, r and θ are the axial, radial and azimuthal coordinates respectively, a is a non-zero constant, and $c(t)$ and $\alpha(t)$ are arbitrary functions of time t. The continuity equation is always satisfied. If we seek a solution with the pressure in the form $p = p(r, z, t)$, and consider the momentum equation, we come to:

$$c(t) = c_0 \exp\left[(a+1)\int_0^t \alpha(t)dt\right], \tag{14}$$

where c_0 is a real constant. The flow field considered in the following is obtained with $a = 2$ and $\alpha(t) = -kt$, with k a real constant. The three velocity components are:

$$u_r = ktr, \qquad u_\theta = c_0 r^2 \exp(-3/2kt^2), \qquad u_z = -2ktz, \tag{15}$$

while the pressure is given by:

$$\frac{1}{\rho}p = \frac{1}{4}r^4 c_0^2 \exp(-3kt^2) - \frac{1}{2}k(1+kt^2)r^2 + k(1-2kt^2)z^2 + C_p. \tag{16}$$

The flow is characterized by a radial velocity which is proportional both to the distance from the axis and to time; by an azimuthal velocity proportional to r^2 and exponentially decaying with time; by an axial velocity proportional to z and time.

A visualization of the flow in a plane normal to the z axis is given in figures 7(a,b); in figure 7(a) the traditional vector plot is used to highlight the geometry of the vortex, while in figure 7(b) curved segments are shown, which have a length proportional to the local instantaneous velocity modulus.

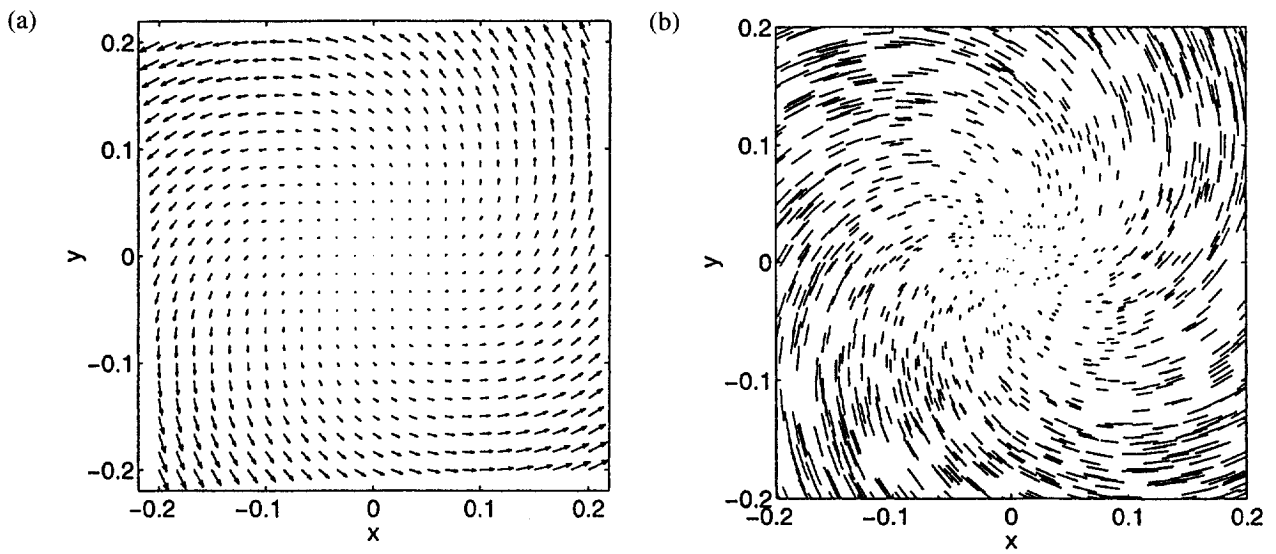

Fig. 7. – Visualization in the plane $z = 0$ at a fixed time of the flow field due to the unsteady inviscid radially stretched vortex. The flow has been computed for the following values of the parameters: $k = 1$, $c_0 = 1$ and $t = 0.1$. (*a*) Vector plot of velocity components. (*b*) Plot of curved streamline segments, of a length proportional to the instantaneous velocity modulus (in the plane considered).

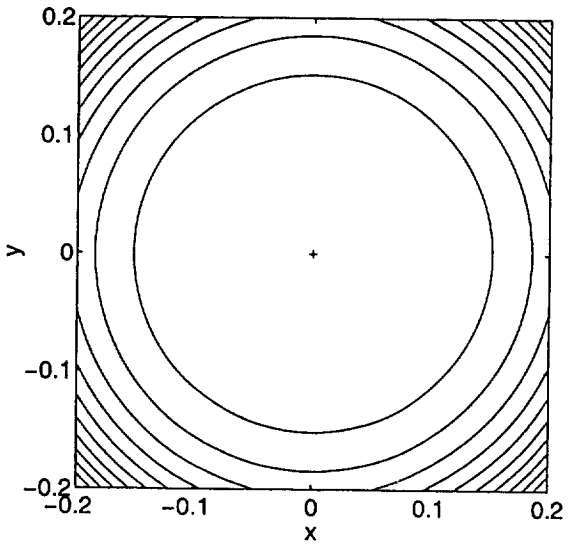

Fig. 8. – Contours of Δ for the unsteady inviscid radially stretched vortex. Parameters as in figure 7. Levels are equally spaced from 0 to 0.0003. The z axis corresponds to $\Delta = 0$.

The computation of the values of Δ in the plane $z = 0$ gives the results shown in figure 8. The detected vortex core (region of positive Δ) lies all over the plane, with the exception of the longitudinal z axis, where $\Delta = 0$ excludes it from the vortex core.

The use of $R(t)$ for the identification of the vortex structure gives the results shown in figure 9(a). Here 10000 particles have been randomly inserted in a slice (0.01 thick) of the flow field, at time $t = 0.1$ and with $k = 1$ and $c_0 = 1$; in this way with $d_m = 0$ and $d_M = 0.003$ we obtain 3091 pairs of particles, which give rise to 2705 pairs with $R < 0.6$. Figure 9(b) is the result of the same calculations, but with $R_{th} = 0.95$ (pairs are

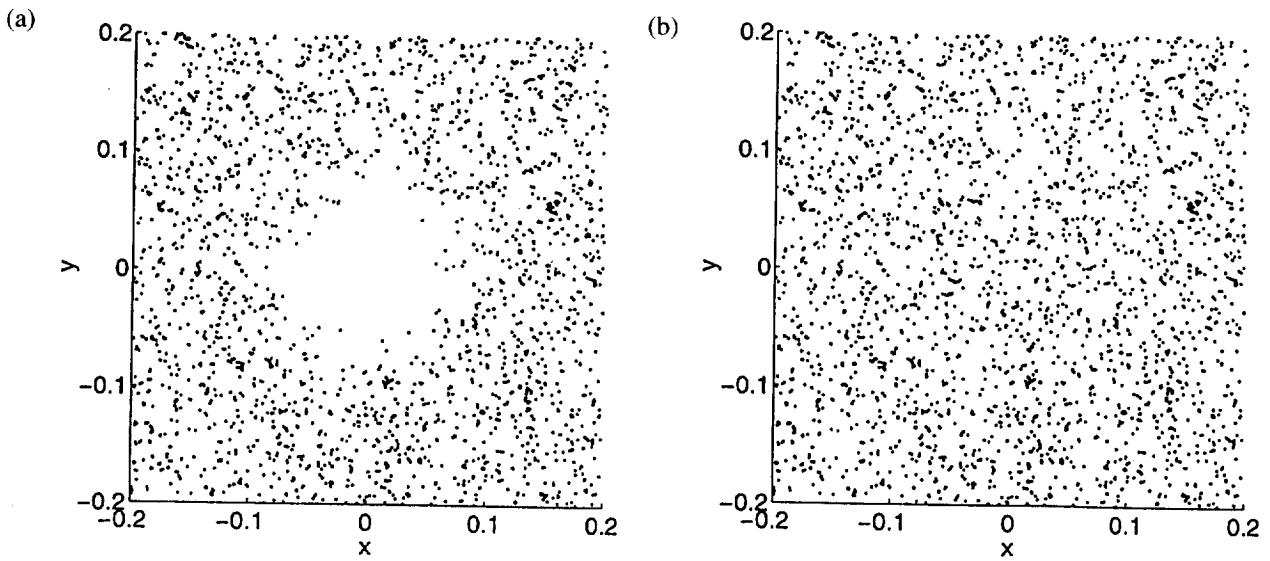

Fig. 9. – Initial positions of the mid point of particle pairs with $R < R_{th}$ in the case of the unsteady radially stretched vortex. Parameters as in figure 7. The integration period is $t = 15$. Pairs followed in pseudo-time are 3091. (*a*) 2705 pairs have $R < R_{th} = 0.6$; (*b*) 3087 pairs have $R < R_{th} = 0.95$.

3087 now). By a comparative examination of figures 9(a) and 9(b) it can be noted that even the $R(t)$ definition detects a vortex core which extends over the full plane, with the exception of the origin: it can be seen that by gradually increasing the value of R_{th} from 0.6 to 0.95 we obtain a gradual reduction of the central region where the procedure only detects particle pairs having $R > R_{th}$.

4.2. Application of Q definition

4.2.1. *The Bödewadt vortex*

This vortical flow Bödewadt (1940), also analyzed by JH, is due to a viscous fluid which possesses a solid-body rotation far from a stationary wall. Away from the wall, there is a balance between the force due to the radial pressure gradient and the centrifugal force. Near the wall, the radial pressure gradient is the same as that present away from the wall, while the centrifugal force decreases because of viscous effects. As a result, near the wall the unbalanced radial pressure gradient moves fluid toward the axis of the vortex, which is normal to the wall; this fluid, by continuity, moves away from the wall. A scheme of this flow is given in figure 10. Velocity components can be written in the following form:

$$u_r = rf(z), \qquad u_\theta = rg(z), \qquad u_z = h(z), \tag{17}$$

and, if Ω is the angular velocity of the solid-body rotation, (17) can be put in the non-dimensional form:

$$\begin{cases} z = (\nu/\Omega)^{1/2}\zeta \\ f(z) = \Omega F(\zeta) \\ g(z) = \Omega G(\zeta) \\ h(z) = (\Omega\nu)^{1/2} H(\zeta). \end{cases} \tag{18}$$

From the Navier–Stokes equations, the unknown functions F, G and H can be then computed with a series expansion.

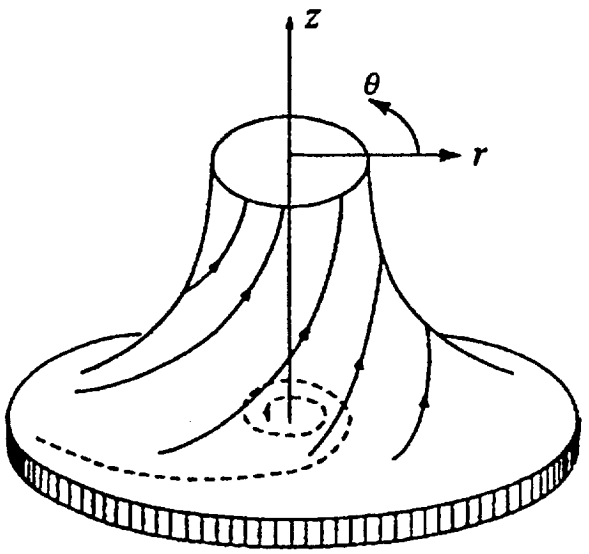

Fig. 10. – Illustration of the Bödewadt vortex (from JH).

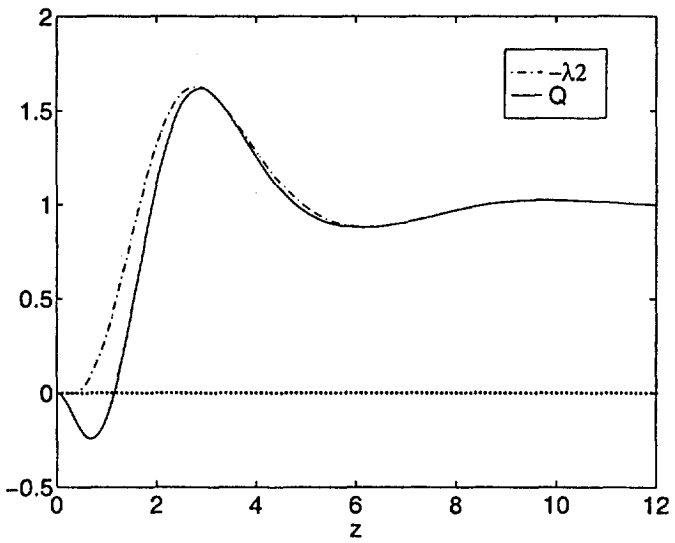

Fig. 11. – Distribution, along the z axis, of Q (continuous line) and $-\lambda_2$ (dotted line) in the case of the Bödewadt vortex.

In figure 11 the continuous line shows the distribution of the quantity Q along the z axis. Near the wall a region can be highlighted (for approximately $z < 1.2$) where the Q-definition does not find any evidence of vortical motion, while it is clear that vortical motion exists down to $z = 0$.

The use of the $R(t)$-definition does not give a result directly comparable with those of figure 11. However, in order to compare results of the different definitions even in this case, figure 12 shows the distribution, along the z axis, of a quantity called pairs density. Pairs density is defined as the number of particle pairs with an initial position of the mid point between z_1 and $z_2 > z_1$, and with $R < R_{th}$, divided by $(z_2 - z_1)$. The integral of this linear density between z_{min} and z_{max} gives the number of pairs having $R < R_{th}$ and with initial position of the mid point between z_{min} and z_{max}. In the case of figure 12, 99.7% of the total number of pairs have $R < 0.6$. If the R-definition were affected by the same problems as those inherent to the Q-definition, the pairs density plotted in figure 12 would show a region for $z < 1.2$ where its value would significantly decrease. This is not the case, since the density of pairs is approximately constant along the z axis: the first point which has been calculated is significantly lower than the others only because it takes into account even the particles very near the wall, which have low velocity due to the no-slip boundary condition, and consequently, for a given integration time, show less variation of R than the outer particles do.

4.2.2. *Unsteady inviscid radially stretched vortex*

The application of the Q-definition to the case of the inviscid, radially stretched vortex described in section 4.1.2 is shown in figure 13. The quantity Q shows a change of sign at a well defined radial position; this suggests that the vortex core does not reach a finite region surrounding the z axis. This is at odds with a direct observation of the flow field.

4.2.3. *Model for a tornado*

Figure 14 shows a contour map of the quantity Q, computed for the tornado flow discussed in section 4.1.1. Q is clearly negative in every point of the flow field; therefore, the conclusions drawn from the present technique are clearly different from those reached from Δ and $R(t)$. For a discussion of the results concerning the tornado flow, see section 4.3.1.

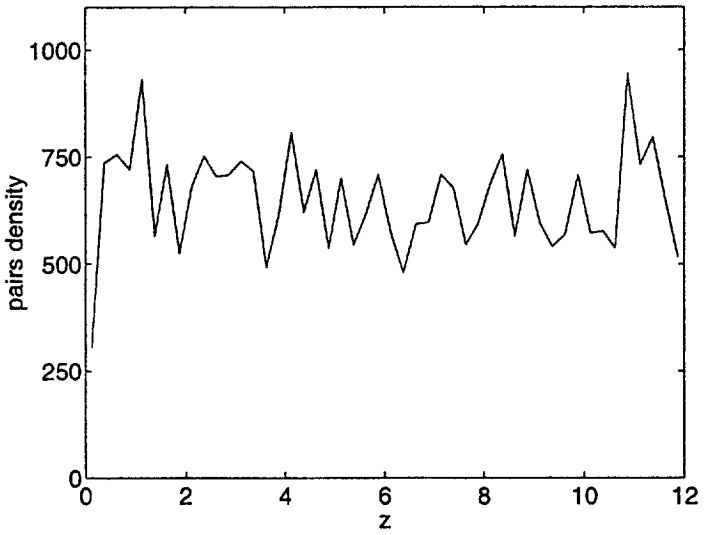

Fig. 12. – Distribution, along the z axis, of pairs density in the case of the Bödewadt vortex. $R_{th} = 0.6$, and the integration period is $t = 12.5$.

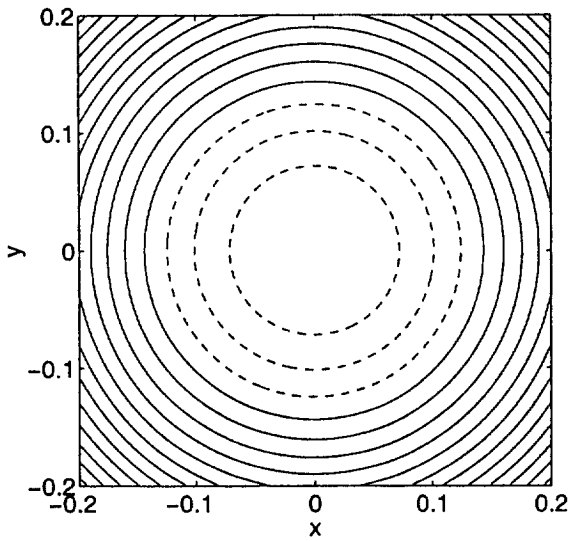

Fig. 13. – Contours of Q for the unsteady inviscid radially stretched vortex. Parameters as in figure 7. Levels are equally spaced from 0.01 to 0.12 (continuous lines) and from -0.02 to 0 (dotted lines).

4.3. Application of λ_2-definition

4.3.1. *Model for a tornado*

The λ_2-definition has been applied to the tornado flow. It is important to note that the example discussed by JH is only apparently similar to the present one. In their paper, JH use a numerical solution of the tornado flow in the one-cell configuration (figure 2(b), and conclude that Δ- and Q-definitions fail in precisely detecting the geometry of the vortex core. On the contrary, in our paper we use an analytical solution of the two-cell flow, which corresponds to the asymptotic case obtained when $\Gamma_0 \to \infty$ (see figure 2(a)).

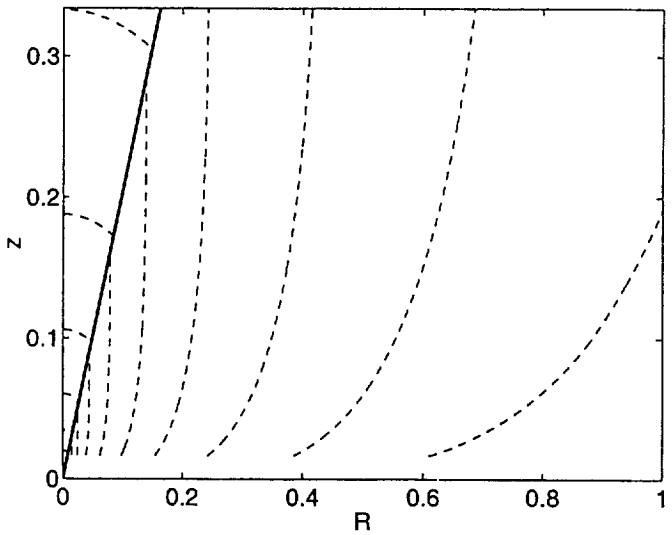

Fig. 14. – Contours of Q in the tornado flow. Parameters as in figure 4. The singular plane $z = 0$ is excluded from the plot. Dotted lines represent negative levels. Thick line corresponds to $\theta = \theta_s$.

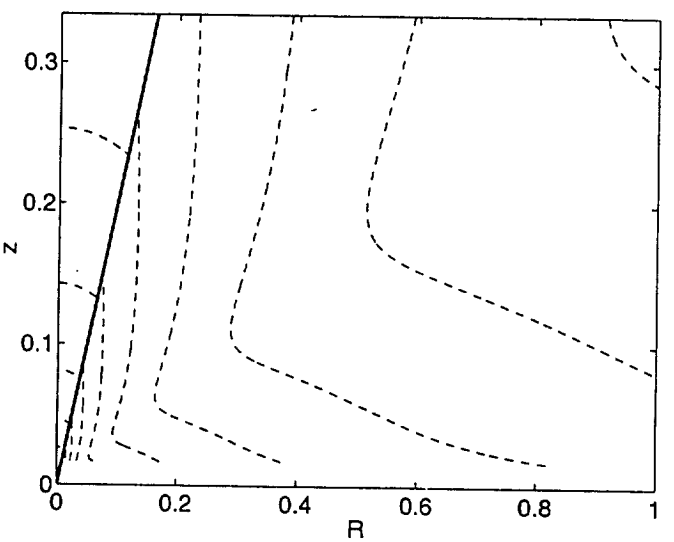

Fig. 15. – Contours of λ_2 in the tornado flow. Parameters as in figure 4. The singular plane $z = 0$ is excluded from the plot. Dotted lines represent positive levels. Thick line corresponds to $\theta = \theta_s$.

A contour map of λ_2 is shown in figure 15. λ_2 takes positive values everywhere, and does not seem to detect any vortex. Hence λ_2 behaves similarly to the scalar Q (figure 14), but differently from Δ, which is able to identify a thin vortical region near $\theta = \theta_s$ (figure 4) .

We must admit that the interpretation of the present flow is not straightforward. If one accepts the idea that the cone at $\theta = \theta_s$ is a vortex sheet, the indications from λ_2 and Q may be correct. On the other hand, even in the asymptotic case, this flow appears to be very close to our intuitive notion of a vortex. We have to bear in mind that we are facing an undoubtedly swirling motion in a rotational region (in section 4.1.1 $\omega_\phi \neq 0$ for $\theta > \theta_s$). According to this, the indications drawn from Δ appear to be acceptable; apart from the region near the plane at $z = 0$ (which however has to be excluded after a deeper observation of the flow, as illustrated

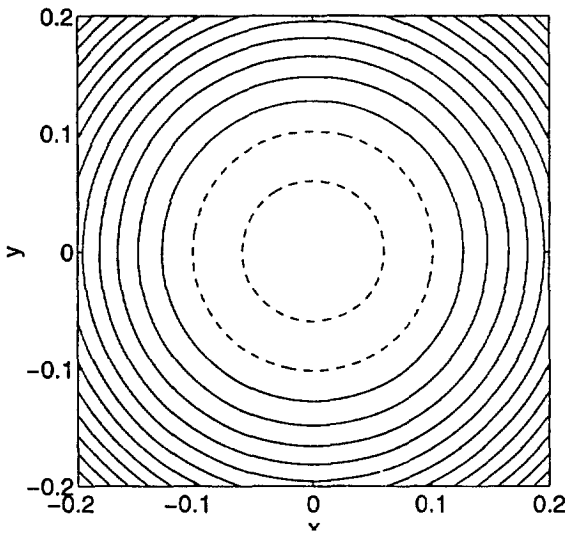

Fig. 16. – Contours of λ_2 in the unsteady inviscid radially stretched vortex. Parameters as in figure 7. Levels are equally spaced from 0 to 0.11 (dotted lines) and from -0.009 to -0.11 (continuous lines).

for example in section 4.1.1), a clearly conical vortex core is detected. The application of the R-definition, reported in figure 6, fully confirms this interpretation, showing a well defined concentration of particles with low values of R near the vortex core.

4.3.2. *Unsteady inviscid radially stretched vortex*

The application of the λ_2-definition provides (figure 16) results very similar to those of Q-definition. Also in this case it is possible to notice a change of sign of λ_2 at a certain radius. For a brief discussion on the similarity between the two quantities Q and λ_2 see the following paragraph. At this point we intend to stress that, although the regions detected by Δ, λ_2 and Q are equal from a topological point of view (at the z-axis $\Delta = 0$, hence the axis is excluded from the vortical region), in this case the Δ-definition allows us to evaluate a shape of the vortex core which is nearer to that suggested by the direct observation of the flow. This can be a very interesting feature, when such techniques are applied to flow fields (e.g. computed by direct numerical simulations) where the actual vortical structures are not known in advance.

As a final remark, let us say that also the R-definition gives indications which are coherent with that of Δ.

4.3.3. *The Bödewadt vortex*

The distribution of $-\lambda_2$ along the z axis in the case of the Bödewadt vortex is shown with a dotted line in figure 11. It is evident that the λ_2-definition is not affected by the problems manifested by Q-definition. The two methods behave differently near the wall, whereas far from the wall the values of the scalars tend to be equal. In order to understand this point, it is worth remembering that Q results from a total balance between rotation and deformation rates of an infinitesimal fluid element, which is positive when the former prevails and negative when the latter prevails. A viscous fluid flowing near a wall is characterized by high values in the deformation rate and, consequently, Q can turn out to be negative even in presence of a vortical structure. The λ_2-definition, on the other hand, carries out the balance between rotation and deformation rates on three distinct planes. We have seen in section 3.1 that, in a reference frame aligned with the eigenvectors of $\mathbf{S}^2 + \mathbf{\Omega}^2$, λ_2 can be negative only if ω_1^2 is sufficiently greater than γ_1^2. In the case of the Bödewadt vortex, the λ_2-definition can precisely locate the vortex core because it carries out selective balances. On the contrary the Q-definition fails, because

the distortion associated with strains parallel to the wall is so great that the global deformation rate prevails over the global rotation rate. This is the reason why Q and $-\lambda_2$ tend to the same numerical value far from the wall. In fact for high values of z the flow tends to a solid-body rotation where the two kinds of balance are equivalent.

5. Discussion and conclusions

In this work, some recently proposed criteria for the identification of vortices have been discussed. Special emphasis has been given to the physical meaning and implications of such criteria. In addition to this, a new approach to the topic has been proposed.

A first method (Chong *et al.*, 1990) deals with complex eigenvalues of the tensor $\nabla \mathbf{u}$, which exist when the discriminant Δ of equation (1) is positive. This method has been illustrated and applied to some flow fields, and a way to interpret the results provided by this technique has been proposed; this allows one to identify regions incorrectly indicated by positive values of Δ as vortices.

A second method, (firstly proposed by Jeong and Hussain, 1995) has been considered, which is based on the analysis of the eigenvalues of the tensor $\mathbf{S}^2 + \mathbf{\Omega}^2$. According to this method, a vortex is defined as a region where the intermediate eigenvalue λ_2 assumes negative values. A possible physical interpretation of this procedure, which carries out a local balance between rotation and deformation rates of an infinitesimal fluid element, has been considered more deeply, by pointing out the explicit contribution of the various components of the rotation and strain rate tensors.

This method is similar to a third procedure, proposed by Hunt *et al.* (1988). It also carries out the same balance, but adopts different measures for the rotation and the deformation rates of the fluid element, which leads to the evaluation of the sign of the second invariant Q of the velocity gradient tensor for the identification of a vortex, on the additional condition that the pressure is lower than the ambient value. It has to be noted that, while the Q-definition carries out the balance by comparing global rotation with global deformation rates, the λ_2-definition selects a particular plane where the balance is executed. Consequently, the behavior of the two definitions is similar in many cases.

In any of the previous techniques, at least one counter-example has been given where ambiguous results are obtained. According to the authors' opinion, the reason why this happens is that all the methods mentioned so far carry out a local analysis of the flow field, while vortices are inherently non-local phenomena. Non-local identification techniques (e.g. streamline analysis) often led to non-Galilean invariant algorithms. In this paper, a non-local, Galilean invariant technique is designed. It is based on the computation of a quantity, called R and function of the position and of time, which somehow measures the tendency of two particles in the flow to remain near each other; R consequently offers a quantitative way of characterizing the trajectories of two particles inside a vortical structure. $R(\mathbf{x}, t)$ has been computed for every flow field analyzed using the other techniques, and the results are promising. Additionally, the computation of R presents the remarkable advantage of not requiring the computation of derivatives: this can be very useful when applying these methods to flows that present discontinuities. It is probably not a coincidence that this technique gives results always in agreement with those from the combined use of Δ-definition and its extension described in section 3.3; in this way both the procedures are based on a non-local analysis.

The extension of the procedures analyzed in the present work to non-constant property flows is straightforward. Even the physical interpretation of the different methods is the same, with the only exception of the λ_2-definition. In this case, we have reported in the appendix the relation between the Hessian of the pressure and the tensor $\mathbf{S}^2 + \mathbf{\Omega}^2$. It can be seen that the use of $\mathbf{S}^2 + \mathbf{\Omega}^2$ as an approximation of $p_{/ij}$ requires dropping other terms beside those left out in the case of incompressible flow, i.e. besides unsteady straining and viscous effects.

The use of local procedures often leads to the selection (more or less explicit in the different methods) of a particular privileged direction, which is considered the vortex axis (see e.g. JH in their abstract). Of the examined methods, this is the case of the λ_2-definition (section 2.4), which takes as privileged direction the direction of the eigenvector associated with the largest eigenvalue of $\mathbf{S}^2 + \mathbf{\Omega}^2$; less evidently, even the Δ-definition (see Chong *et al.*, 1990, section III) considers as a privileged direction the direction of the eigenvector associated with the real eigenvalue of the tensor $\nabla \mathbf{u} = \mathbf{S} + \mathbf{\Omega}$. These directions, which coincide only when the two definitions both detect a vortex, are often associated with the concept of the vortex axis; it has to be said, however, that in general they are different at any point inside a vortical structure. Q- and R-definitions, on the other hand, do not rely on a particular direction.

In conclusion, we can say that none of the methods considered here can be regarded as the definitive solution to the problem of vortex identification. Nevertheless, an appropriate use of these methods permits one to obtain useful information even from complex flow fields. In our opinion, improvements in such techniques can be achieved by exploiting the intrinsic *non-locality* of the vortical structures.

Acknowledgements. – The authors wish to thank Professor Paolo Luchini for the stimulating discussions about the concept of persistency of vortical structures. This work has been partially supported by the M.U.R.S.T in the year 1993-1994.

APPENDIX

Pressure Hessian in the case of a compressible fluid

The Navier–Stokes equations, written for a compressible fluid with constant viscosity, are:

$$\rho(u_{i/t} + u_k u_{i/k}) = -p_{/i} + \mu u_{i/kk} + (\lambda + \mu) u_{k/ik}. \tag{19}$$

Let us first take the gradient of (19) by deriving it with respect to the direction j:

$$\begin{aligned} &\rho(u_{i/jt} + u_{k/j} u_{i/k} + u_k u_{i/jk}) \\ &\quad = -p_{/ij} + \mu u_{i/jkk} + (\lambda + \mu) u_{k/ijk} - \rho_{/j}(u_{i/t} + u_k u_{i/k}). \end{aligned} \tag{20}$$

The symmetric part of (20) can be obtained by applying to it the operator $1/2\big((\cdot)_{i/y} + (\cdot)_{j/i}\big)$, and results in:

$$\begin{aligned} &\frac{1}{2}\rho(2S_{ij/t} + u_{k/j} u_{i/k} + u_{j/k} u_{k/i} + u_k u_{i/jk} + u_k u_{j/ik}) \\ &\quad = -p_{/ij} + \mu S_{ij/kk} + (\lambda + \mu) u_{k/ijk} - \frac{1}{2}\left(\rho_{/j}\frac{\mathrm{D}u_i}{\mathrm{D}t} + \rho_{/i}\frac{\mathrm{D}u_j}{\mathrm{D}t}\right) \end{aligned}$$

where $S_{ij} = 1/2(u_{i/j} + u_{j/i})$ and $\Omega_{ij} = 1/2(u_{i/j} - u_{j/i})$. By substituting:

$$\frac{1}{2}(u_{k/j} u_{i/k} + u_{j/k} u_{k/i}) = S_{ik} S_{kj} + \Omega_{ik} \Omega_{kj}$$

$$S_{ij/t} + \frac{1}{2}(u_k u_{i/jk} + u_k u_{j/ik}) = \frac{\mathrm{D}S_{ij}}{\mathrm{D}t}$$

we obtain the final expression:

$$\rho\frac{\mathrm{D}S_{ij}}{\mathrm{D}t} + \rho(S_{ik}S_{kj} + \Omega_{ik}\Omega_{kj}) - \mu S_{ij/kk} + - (\lambda+\mu)u_{k/ijk} + \frac{1}{2}\left(\rho_{/j}\frac{\mathrm{D}u_i}{\mathrm{D}t} + \rho_{/i}\frac{\mathrm{D}u_j}{\mathrm{D}t}\right) = -p_{/ij}. \tag{21}$$

In comparison with the equivalent expression (3) derived by JH in the case of incompressible flow, we can note the presence of additional terms in the expression of the Hessian $p_{/ij}$ of the pressure. The last two terms in the left hand side of (21) are indeed related to the presence of a non-zero divergence, and to non-zero density gradients respectively.

REFERENCES

BÖDEWADT U.T., 1940, Die Drehströmung über festern Grund, *Z. Angew. Math. Mech.*, **13**, 141.

CANTWELL B.J., 1981, Organized motion in turbulent flow, *Annu. Rev. Fluid Mech.*, **13**.

CHONG M.S., PERRY A.E., CANTWELL B.J., 1990, A general classification of three-dimensional flow field, *Phys. Fluids* **A 2**, 765.

HUNT J.C.R., WRAY A.A., MOIN P., 1988, Eddies, stream and convergence zones in turbulent flows, *Center for Turbulence Research Report CTR-S88*, 193.

HUSSAIN F., 1986, Coherent structures and turbulence, *J. Fluid Mech.*, **173**, 303.

KLINE S.J., ROBINSON S.K., 1990, Turbulent Boundary Layer Structure: Progress, Status and Challenges, *Structure of Turbulence and Drag Reduction*, ed. A.Gyr, Springer.

JEONG J., HUSSAIN F., 1995, The identification of a vortex, *J. Fluid Mech.*, **285**, 69–94.

JEONG J., HUSSAIN F., SCHOPPA W. & Kim, J., 1997 Coherent structures near the wall in a turbulent channel flow. *J. Fluid Mech.* **332**, 185–214.

PERRY A.E., CHONG M.S., 1987, A description of eddy motions and flow patterns using critical-point concepts, *Annu. Rev. Fluid Mech.*, **19**, 125–155

ROBINSON S.K., 1991, Coherent motions in the turbulent boundary layer, *Annu. Rev. Fluid Mech.*, **23**, 601–639.

SHTERN V., HUSSAIN F., 1993, Hysteresis in a swirling jet as a model tornado, *Phys. Fluids*, **A 5**, 2183.

SHTERN V., HUSSAIN F., 1996, Hysteresis in swirling jets, *J. Fluid Mech.*, **309**, 1.

SPALART P.R., 1988, Direct simulation of a turbulent boundary layer up to $R_\theta = 1410$ *J. Fluid Mech.*, **187**, 61–98.

TRUESDELL C., 1953, *The kinematics of vorticity*, Indiana University, Indiana, USA.

(Received 6 June 1997;
revised 14 July, 1998;
accepted October 1998.)